THE GRUMMAN/BROOKHAVEN HIGH-BRIGHTNESS, HIGH-DUTY FACTOR RF GUN*

I.S. Lehrman, I.A. Birnbaum, M. Cole, S.Z. Fixler, R.L. Heuer, S. Siddiqi, E. Sheedy
Grumman Corporate Research Center, 4 Independence Way, Princeton, NJ 08540

I. Ben-Zvi, K. Batchelor, J.C. Gallardo, H.G. Kirk, T. Srinivasan-Rao
Brookhaven National Laboratory, Upton, NY 11973

G.D. Warren
Mission Research Corporation, 8560 Cinderbed Road, Newington, VA 22122

Abstract

Under a joint collaboration between the Brookhaven National Laboratory and the Grumman Corporation, a high-duty factor (>1%) photocathode RF gun is under construction for use at the ATF facility at BNL. The gun will be capable of producing short (< 6 psec) bunches of electrons at high repetition rates (5 kHz), low energy spread (< 1.0%), peak currents of > 300 A (after compression) and a total bunch charge in excess of 3 nC. The gun consists of 3-1/2 cells constructed from GlidCop, an alumina dispersion strengthened copper alloy. Two individually phased waveguides are used to power the first two and final two cells.

Introduction

The free-electron laser (FEL) offers the opportunity of providing high power coherent radiation sources in regions presently unattainable by conventional atomic and molecular lasers. For this reason, it has been proposed to build an ultraviolet FEL users' facility[1] capable of producing radiation between 75 – 300 nm at a repetition rate of 5 kHz. Though the superconducting linear accelerator for this facility is considered to be proven technology, the RF photocathode gun would be operating in a regime undemonstrated at this time. The gun would be required to produce 2 pulses separated by 10 ns every 200 μsec. The emittance of the electron bunches is required to be below 7π mm-mrad (normalized RMS) with peak currents of 300A after compression. The RF filling times of these guns are on the order of $1 - 2$ μsec, thus the RF duty factor would be nearly 1%. In addition to FELs, RF guns are well suited for the front ends of a number of accelerators which require high-current, short-pulse beams (i..e. beamlines for pulse radiolysis, the Next Linear Collider).

The construction of such a gun (Gun II) has begun under a joint Grumman-Brookhaven National Laboratory (BNL) research collaboration. The starting point for our design is the present 1-1/2 cell BNL photocathode RF gun (Gun I) shown in Fig. 1. The beam dynamics of the gun were modeled with the PARMELA [2] and MAGIC [3] particle codes. These codes are used to study the emittance growth of the electron bunch as it is accelerated through the gun, as well as to determine how the operational parameters effect its characteristics (i.e. divergence, momentum spread, energy, current).

The thermal and mechanical properties of the gun were modeled with the ANSYS [4] finite element code. Power deposition profiles were calculated with SUPERFISH [5]. A thermal/structural analysis was performed to determine the temperature profiles and the pressure and thermally induced
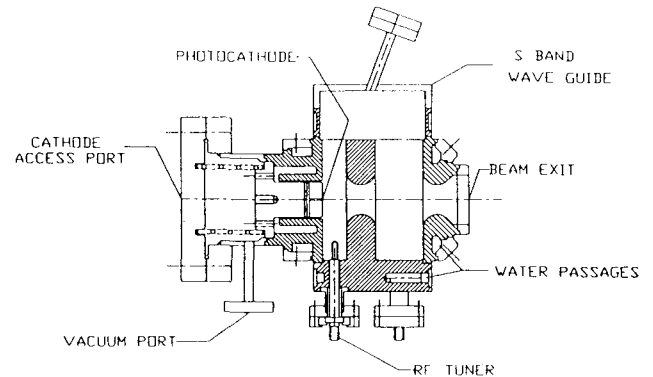
Figure 1. Present BNL 1-1/2 cell gun (Gun I).

stresses. The Von Mises (equivalent) [6] Stress Criteria were used to determine the stress level margins.

Beam Dynamics Modeling

The majority of the beam dynamics modeling was done with the MAGIC particle-in-cell code. This code includes the effect of image currents, space charge and wakefields. The axisymmetric gun geometry (2D) was modeled with the exact gun fields. This is accomplished by prescribing the magnetic field for the fundamental TM_{01} cylindrical cavity mode and allowing the cavity to ring while numerically damping out higher order modes. The ratios of the electric and magnetic fields are compared at various times to verify that the higher order modes are greater than 60 dB down from the fundamental mode. The fields are then stored and used for later runs with particles. The damping of higher order modes is turned off for the particle runs. Fig. 2 shows a vector plot of the electric fields for a 3-1/2 cell gun.
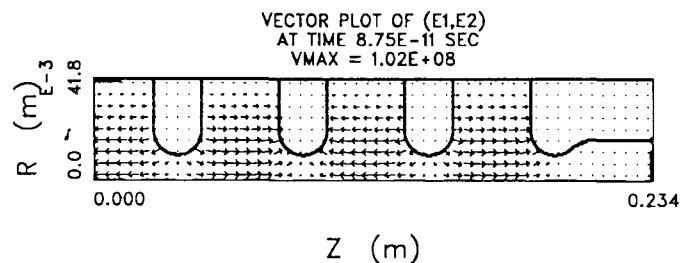
Figure 2. Vector plot from MAGIC of the electric field in the 3-1/2 cell gun (Gun II)

The advantage of using the MAGIC code is that the field components at the cavity apertures and beam exit are continuous and the method of calculating the space charge forces is inherently more stable. To properly resolve the electric fields of the electron bunch near the cathode, where they are rapidly accelerated, the numerical grid for calculating the fields is made very fine near Z, R = 0. In addition, the time steps are small enough to avoid plasma frequency and grid type instabilities, and to properly resolve the temporal behavior of the wakefields[7]. Typical simulations for a 3-1/2 cell gun consisted of a grid 2000 x 90 (Z x R) with 1500 particles. Particles are emitted in nearly any functional form in radius and time to model the laser illumination of the cathode.

The majority of our simulations used Gaussian profiles with a temporal extent of $\pm 2\sigma_t$ (σ_t = 2 psec), and a radial extent of $1\sigma_r$ ($\sim 1 - 5$ mm). Table 1 lists the operational parameters for Gun II. Statistics of the particles are tracked through the length of the gun. The emitted electron bunch could be modeled as initial cold ($\varepsilon_n = 0$), or thermalized (by an amount equal to the difference between the photon energy of the laser and the work function of the cathode material). The most recent experiments at BNL[8] have utilized a copper photocathode whose work function is better matched to the photon energy of the laser than the previous Yttrium cathode. The thermal energy for electrons emitted from the Cu cathode is 0.4 eV versus 1.5 eV for the Yt cathode. To improve the resolution of space charge and RF emittance contributions, the particles were emitted cold in the majority of our simulations. Emittance values are always reported with the addition (in quadrature) of the thermal emittance.

Table 1. Operational parameters of Gun II

Number of cells	1
Laser radius ($1\sigma_r$)	4 mm
Pulse length ($\pm 2\sigma_t$)	8 psec
Cathode electric field (nominal)	100 MV/m
Beam momentum	10 MeV/c
Peak power	12.5 MW
Duty factor	1%
RF frequency	2.856 GHz

Most of our simulations were done for a 1-1/2 cell gun since they require 1/4 of the computer time and uncover most of the underlying physics. A number of aspects of the gun design were investigated: temporal and spatial laser illumination profile shaping; total charge; electric field strength; launch phase; field tilt; aperture shaping; and the length of the first cell. The brightness, B, was used as one figure of merit for our gun design. We use the definition:

$$B = \frac{I}{\varepsilon_n^2} \ , \ I = \frac{Q}{\sqrt{2\pi} \ \sigma_b},$$

where I is the peak current, ε_n is the RMS invariant emittance, Q is the total charge, and σ_b is the bunch length (divided by the speed of light). After the beam exits the gun, it enters a transport line whose function is to match the beam to the linac. In addition, the transport line may serve to magnetically compress the bunch length, resulting in peak currents >1000

amps. The compression results from differing path lengths for particles of differing momentum in bending magnets. The compressibility was determined analytically and used to determine the ideally compressed current.

The divergence of the beam is inversely proportional to γ, the relativistic factor, and the space charge forces are inversely proportional to γ^2. Simulations of the full 3-1/2 cell gun show that the addition of 2 full cells for the gun (Gun II) will double the momentum of electrons to 10 MeV/c which should result in a bunch that is more easily transported and compressed.

A study was made to determine the effect of varying the length of the half cell on the emittance, divergence and compressibility. It was found that by increasing the length of the half cell from 2.625 cm (λ/4) to 3.5 cm, the divergence was reduced by 20%, the compressibility increased by a factor of 2, and the effect on the emittance was negligible. The 3.5 cm first cell offers a number of other advantages. The peak electric field is on the cathode rather than on the aperture as in the previous case. This should allow the cathode field to reach 110 MV/m with the same conditioning that it takes to reach 100 MV/m in the present BNL gun.

A number of post-processing utilities were developed for the MAGIC code to uncover the underlying causes of emittance growth in the gun. Fig. 3 shows the longitudinal phase space (1 nC bunch) at the gun exit ($\sigma_b = 0.55$ mm, dP/P = 1.5%) and after being ideally compressed ($\sigma_b = 0.029$ mm). Figure 4 shows the transverse phase space at the gun exit ($\sigma_r = 4.9$ mm, $\sigma_r' = 11.7$ mrad). Figure 5a shows the transverse phase space deviations which are defined by:

$$\dot{r}_{new} = \dot{r}_{old} - \left\langle \frac{r'}{r} \right\rangle r_{old}$$

where <r'/r> is determined from the particle ensemble. The deviations indicate that the front and back of the beam are receiving different radial kicks due to the time dependent nature of the RF accelerating field. It appears that by applying a time dependent linear radial kick that the phase space area of the bunch could be reduced, hence lowering the beam emittance. Further investigation shows that the apparent linear slew in the transverse phase space is due to the momentum slew in the longitudinal phase space.

By artificially adding 190 MeV/c to each particle, Fig. 5b shows that the transverse phase space area is already reduced as far as possible. In fact it can be shown that by adjusting the launch phase for minimum emittance, an effective linear kick is imposed on the beam. With this knowledge, it is possible to determine the minimum emittance of the beam without scanning launch phase (as long as you are reasonably close to the correct launch phase).

Fig. 6 shows the slice emittance of the bunch. The slice emittance is the emittance of a small longitudinal section of the bunch. Notice that most of the bunch emittance is below 1π mm-mrad. The tail of the bunch which has the largest emittance can be easily identified in Fig. 5b. By aperturing the bunch in either momentum or physical space, the bunch emittance can be significantly reduced. Another possible way of reducing the bunch emittance is to introduce a quadratic time dependent kick in the transverse phase space. Such a scheme has been proposed by Gallardo[9].

Uncompressed current: 220 amps
Compressed current: 4224 amps
Compression factor: 19.2
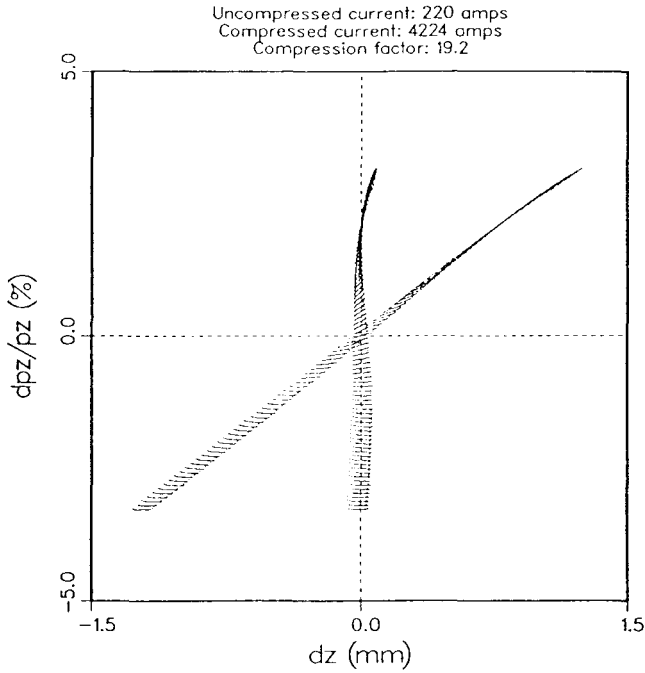
Figure 3. Longitudinal phase space at the exit of Gun II and after ideally compressing the bunch (1 nC).

Transverse phase in r and r
At z = 22.67 cm

r (mm)
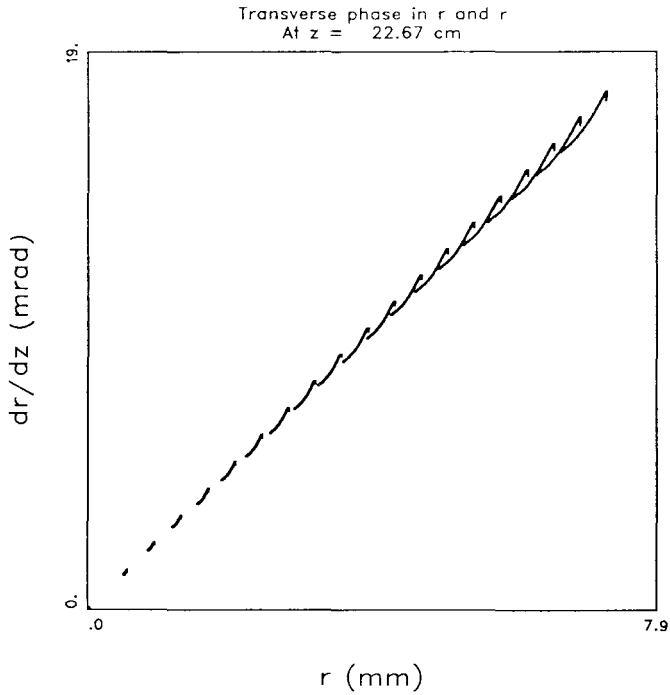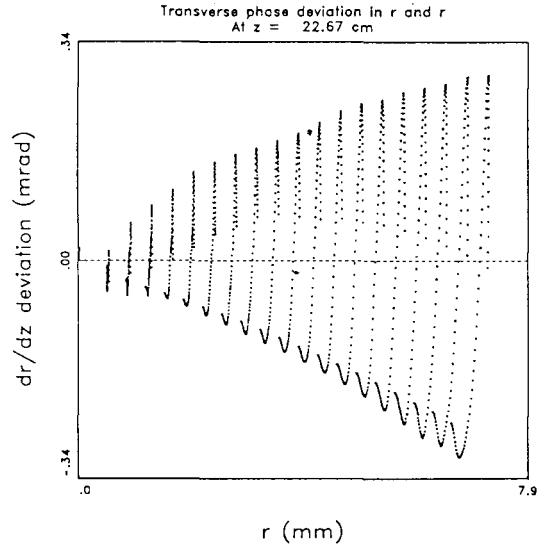
Figure 4. Transverse phase space at the exit of Gun II (1 nC).

Transverse phase deviation in r and r
At z = 22.67 cm

r (mm)

Transverse phase deviation in r and r
At z = 22.67 cm
Accelerated by 190. Mev

r (mm)
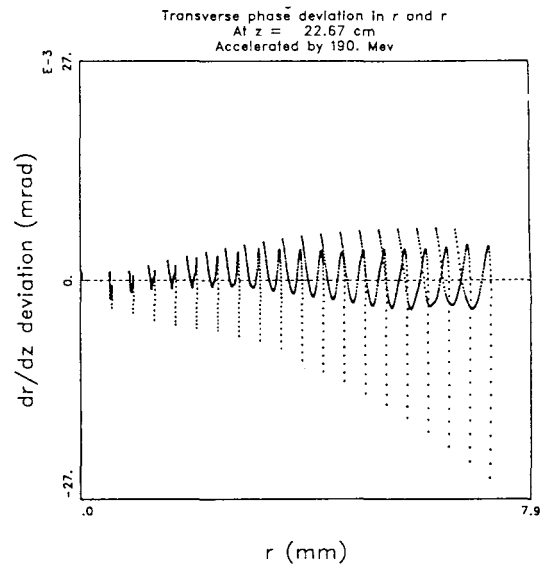
Figure 5. a) Transverse phase space deviations. b) transverse phase space deviations with particles accelerated by 190 MeV/c.

For the gun with the longer half cell, minimizing the emittance requires the launch phase to be advanced by 6° for a 1 nC bunch. If one considers the transit time for a relativistic electron bunch, the extra length of the first cell corresponds to 27° of RF phase. However, since the space charge force greatly influences the front and rear of the beam, the smaller reduction in field provides a time dependent force which acts to counter the repulsive space charge force. As a result, the minimum emittance requires a launch phase advanced by 16° for a 0.1 nC bunch and 6° for a 1 nC bunch.

POSTER processing for emittance vs. z
Total Non-thermal Emittance   2.9 (mm-mrad)
Total Charge   1.0 (nanocoulomb)
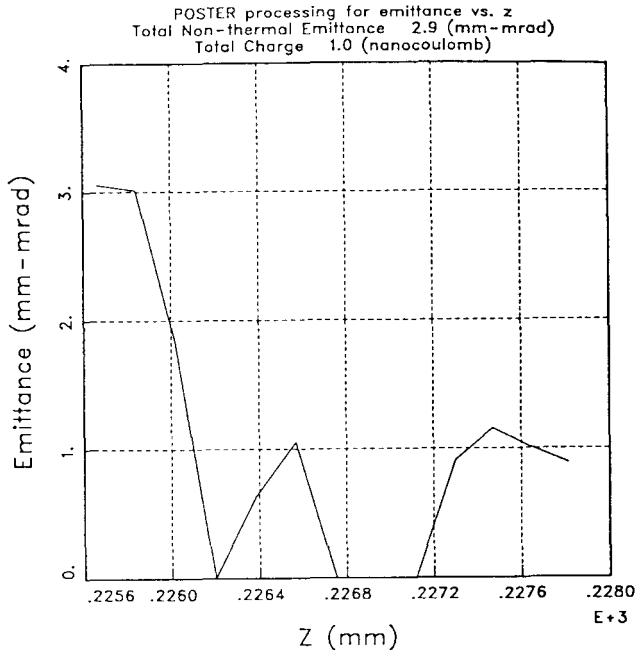
Figure 6. Slice emittance of the beam at the gun exit (1 nC).

The smaller phase advance causes the particles to arrive ahead of the zero crossings at the apertures. The final two cells of the gun will have independent phase control which will compensate for the early of the particles. This provides a means of controlling the longitudinal phase space (decreasing the momentum spread or increasing the compressibility), as well as a means for matching the beam to the compression system. Table 2 summarizes the beam dynamics modeling for Gun II.

Table 2. Modeling results for Gun II

Charge (nC)	0.5	1.0	3.0
Emittance (π mm-mrad)	2.3	3.4	8.9
Divergence (x' mrad)	7.9	8.3	9.5
Momentum spread	~ 0.2%	− 2.0%	(selectable)
Launch phase	55°	59°	63°
Peak current			
Uncompressed (A)	118	220	571
Compressed (A)	2705	4224	7429

Thermal and Mechanical Design

Operation at duty factors of 1% present significant challenges in the heat removal aspects of the gun as well as the pressure and thermally induced stresses and deformations. The half cell of the gun will be 3.5 cm long followed by 3 full cells each 5.25 cm ($\lambda/2$) in length. The longer cell simplifies the construction of the gun by reduced the space constraints. Fig. 7 shows a cut away view of Gun II.
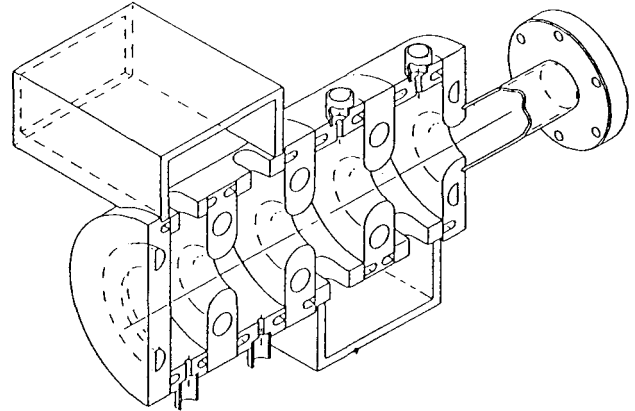
Figure 7. Cutaway view of Gun II showing the locations of the water cooling channels.

The peak power in the gun is 12.5 MW, thus an average power of 125 kW most be removed from the structure. Since Gun II will utilize a copper cathode, the cathode wall will be constructed of a solid copper plate without penetrations. The cathode plate, four cylindrical spool pieces and four aperture pieces will be brazed together. The cathode plate is a 0.75 cm long cylinder 12.25 cm in diameter, with coolant channels milled in a circular pattern. A second 0.75 cm long cylinder is brazed on the back to enclose the channels. A 2.5 cm long cylindrical spool piece is used to connect the photocathode to the aperture. The spool pieces for the full cells are 3.25 cm long. All of the spool piece are cooled by circular channel machined into each end. Each aperture is designed as two cylindrical pieces, 1.0 cm long with two coolant channels milled in a circular pattern, which are brazed together. The aperture opening is a separate machining operation.

We have chosen to use GlidCop-25, an aluminum oxide dispersion strengthened copper alloy, which combines good thermal, electrical, and structural properties. The GlidCop will be electroplated with 0.001" of OFHC copper to provide the good electrical conductivity for the cavity and a barrier for the silver based braze alloys.

The Swanson Analysis System, ANSYS, was chosen as the finite element thermal/structural code to perform the evaluation of the design. ANSYS provides 2-D and 3-D modeling capability with thermal and structural elements compatible with the analysis requirements. Steady state and transient analysis with temperature dependent material properties can be performed.

The thermal management of the gun requires heat removal from a cavity only 8.31 cm in diameter with peak power densities of 22 kW/cm^2. The mode of heat transfer chosen is turbulent forced convection, the Dittus-Boelter heat transfer correlation was used. The heat removal is provided by pumping pressurized water through strategically placed coolant channels. Pressure drops through the channels were addressed, to ensure that boiling does not occur, and to comply with facility capabilities. The flow rates were limited by erosion considerations. Flow velocity limits for copper were within the recommended guidelines.[10]

The power density was supplied by the SUPERFISH code for the cavity configurations evaluated. The power density in the longer half cell is decreased by nearly 15%. Various 2-D axisymmetric models of the gun were generated to determine flow rates, and the positions and sizes of the coolant channels. Steady state thermal analysis was performed for the various evaluations. The operating pressure and temperature distributions are input to the structural model and the pressure and thermally induced deformations and stresses are calculated. The resulting displacements are evaluated to determine the variation in cavity deformations impacting the frequency and tuning of the cavity. The stresses are evaluated and compared to the various stress categories in the ASME Boiler and Pressure Vessel Code. The combination of the stresses used for comparing the ASME allowables are conservative, since they include the thermally induced membrane stress in the Primary+Bending stress category, and the peak thermal stresses in the Primary+Secondary stress category.

The temperature distribution (3-D) shows that the peak temperature of the gun should reach about 144 °C which corresponds to a frequency shift of 4.4 MHz. The maximum Von Mises stress is less than 21 ksi (145 MPa) with an allowable of 31 ksi (214 MPa). 3-D modeling indicates no significant increases in either the temperatures or stresses occur near the coupling slots. Though these stress levels are well within the allowable levels for GlidCop, they exceed the allowable levels for OFHC copper (Yield Stress = 11 ksi).

RF Dynamics

The design of Gun II requires that π-mode phasing be maintained between cells 1 and 2 and between cells 3 and 4. In addition, we would like to vary the phase smoothly between cells 2 and 3. The arrangement of the coupling slots and the distance of the waveguide short from the coupling slots ($\lambda/4$) preferentially couples to the π-mode. Figure 8 shows the mode separation and relative amplitudes for the 0 and π-modes when two adjacent cells are driven with a single loop coupler or with the waveguide. Notice that the single loop excites the 0-mode most strongly by aperture coupling to the second cavity. By comparison, the waveguide most strongly excites the π-mode. The coupling constant is approximately 5×10^{-4}.

Although the coupling is relatively small, it is too strong to allow independent phasing of the two waveguide feeds. Since Gun II will be feed from a single klystron, it is necessary to be able to adjust the phase shifter without changing the waveguide match or the resonant frequency of the coupled system.

We will reduce the coupling between cells 2 and 3 by modifying the aperture between the two cells. This will entail either reducing the diameter of the aperture or increasing the thickness of the aperture. We are presently performing measurements of a cold model to determine the best choice. In order to match the waveguide to the gun, the coupling slots most be sized for critical coupling. The coupling is dependent on the Q of the cavity, therefore, the coupling slots will be slightly undersized and the gun will be brazed together. The final matching of the waveguide to the gun will then be achieved by shimming the height of the waveguide above the
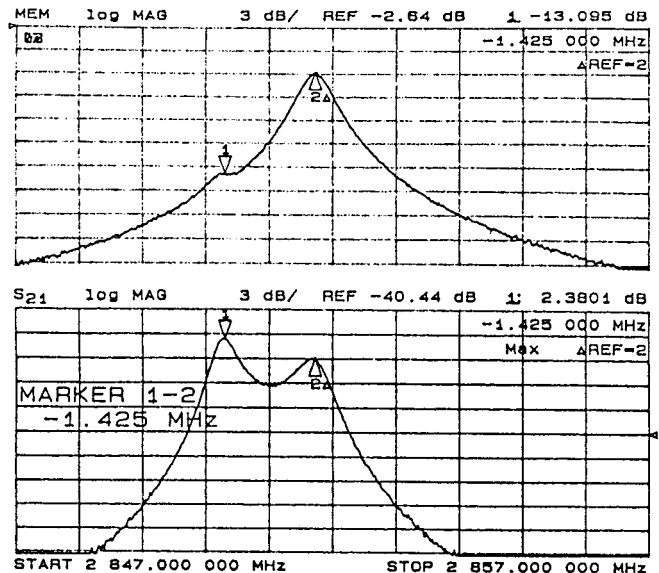
Figure 8. Network analyzer plots of the mode structure in Gun II. Points 1 and 2 indicate the locations of the 0-mode and π-modes, respectively. Waveguide driven (top) and loop driven (bottom).

coupling slots. This method is preferred over cutting the coupling slots since the resonant frequency of the cavity is significantly influenced by the size of the coupling slots.

References

[1] I. Ben-Zvi, L.F. Di Mauro, S. Krinsky, M.G. White and L.H. Yu, Nucl. Instr. and Meth. A304 (1991) 181.
[2] K. R. Crandall and L. Young, PARMELA, in: The Compendium of Computer Codes for Particle Accelerator Design and Analysis, eds. H. Deaven and K.C. Chan, Los Alamos Natl. Rep. La-UR-90-1766 (May 1990) 137.
[3] G.D. Warren, L. Ludeking, J. McDonald, K. Nguyen and B. Goplen, Proc. Conf. on Computer Codes and the Linear Accelerator Community, Los Alamos National Laboratory, Jan 22–25, 1990, ed. R. Cooper, LA-11857-Z (1990) 57.
[4] ANSYS engineering analysis system, Rev 4.3A, Swanson Analysis Systems Inc. Houston, Pa. (1987).
[5] M.T. Menzel and H.K. Stokes, Users guide for the POISSON/SUPERFISH group of codes, Los Alamos Natl. Lab. Rep. LA-UR-87-15 (Jan. 1987).
[6] E.F. Bruhn, Equivalent stress theory, Analysis and Design of Flight Vehicle Structures, Part C (Tri-State Offset Co., Cinn., OH, 1965).
[7] C. K. Birdsall and B Langdon, "Plasma Physics Via Computer Simulation," McGraw-Hill, New York (1985).
[8] K. Batchelor et al., Nucl Inst and Methods A318 (1992) 372.
[9] J. Gallardo and R. Palmer, Nucl. Instr. and Meth. A304 (1991) 345.
[10] G. Stoner, "A Report on Corrosion Engineering Services for the Temperature Control of the ATS and ATSU Accelerator Systems for LANL," Los Alamos internal report (1985)